

NONELASTIC EFFECTS ON THE FAST NEUTRON SPECTRUM IN PB-208

James Paul Holloway
University of Michigan
2355 Bonisteel Boulevard
Ann Arbor, Michigan 48109-2014
hagar@umich.edu

Keywords: lead moderator, neutron spectrum, accelerator driven

ABSTRACT

The problem of neutrons slowing down in Pb-208 from somewhat above the inelastic scatter threshold is examined. Monte Carlo simulations show a significant flux depression immediately below the source energy. This flux depression is explained using analytical information extracted from the neutron slowing down equation. It is shown to be the result of continuous elastic slowing down in competition with nonelastic slowing down events such as inelastic scatter and $(n, 2n)$ reactions. The analytical model recovers the qualitative features of the Monte Carlo simulations. The essential features of the theory apply to neutrons slowing down in other heavy elements, such as Bismuth, although in most other cases the inelastic scatter physics is more complex.

1 INTRODUCTION

There is increasing interest in lead and lead-bismuth moderated reactor systems (Gromov *et al.*, 1996, 1997), especially for the accelerator driven subcritical energy amplifier concept (Andriamonje *et al.*, 1995; Bacher, 1999; Carminati *et al.*, 1993) and in the accelerator transmutation of waste (Van Tuyle *et al.*, 2001). The flux of neutrons slowing down from a monoenergetic source is the Greens function for neutron slowing down problems, and thus provides an important concrete representation of the effects of neutron slowing down physics. In this paper I will describe an interesting feature of this Greens function for neutrons slowing down above the inelastic scatter threshold in pure Pb-208. The general ideas will apply to other heavy moderators as well.

For energies even up to 150 MeV we can, perhaps complacently, compute the neutron slowing down spectrum with any of a number of Monte Carlo codes, such as MCNP (Briesmeister, 2000) and MCNPX (Waters, 1999), using evaluated data created for the accelerator production of tritium project (Chadwick *et al.*, 1999). Below 20 MeV standard ENDF-B/VI evaluations are also widely available. But actually understanding the results from such a Monte Carlo is another matter. The characteristic feature of neutron slowing down in lead is the tiny energy loss in elastic scatter, leading to an excellent and often used description by continuous slowing down theory (Beckurts and Wirtz, 1964). This continuous slowing down has even recently been proposed as an important property in transmuting fission products and fissioning actinides (Abánades *et al.*, 1995) in lead

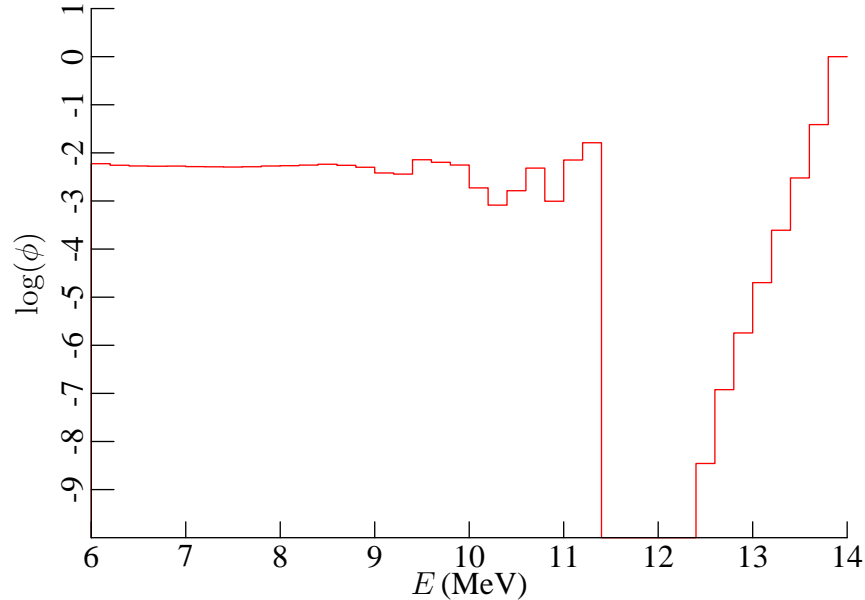


Figure 1: The neutron spectrum generated by 14 MeV neutrons slowing down in Pb-208; computed using 2×10^8 particles in MCNP. Note the large flux depression just below the source energy.

moderated systems, because as it continuously slows down every neutron gets a chance to interact in every resonance. But this intuition about neutrons slowing down in the keV energy range does not help us when considering higher energy neutrons.

Imagine this: 14 MeV neutrons are injected into an infinite medium of pure Pb-208. If these neutrons simply slowed down continuously due to elastic scatter then the flux would behave monotonically like $1/E$, achieving a minimum at the source energy. Reality is more interesting; there will in fact be a local maximum at the source energy and a very deep minimum a few MeV below it, followed by a very sudden increase of neutrons with decreasing energy.

Figure 1 shows the neutron spectrum produced by a 14 MeV neutron source in an infinite mass of Pb-208; this spectrum was computed using 2×10^8 source neutrons in MCNP. Note the huge flux depression just below the source energy; several energy bins—those for which no data is shown—had *no* simulation neutrons enter them. At first sight this strange flux depression might suggest a defect in the code, but it is in fact good physics. While none is so dramatic as this depression in Pb-208, similar flux minima appear in the slowing down spectra for neutrons in other heavy elements including Bi-209, Pb-206, and Pb-207. This paper asserts that such flux depressions are in fact a physical feature of the neutron slowing down spectrum due to a monoenergetic source somewhat above the inelastic scatter threshold in heavy elements. This paper discusses the reason why these flux depressions appear, and presents a simple mathematical model of the flux in such depressions.

2 THE EFFECT OF NONELASTIC EVENTS

The flux depression seen in the spectrum of 14 MeV neutrons slowing down in Pb-208 is caused by a combination of effects:

- Neutrons lose a tiny amount of energy due to elastic scattering from Pb-208 nuclei, and must therefore elastically scatter many times to move appreciably below the source energy. . .
- or at least they would, if the competing nonelastic processes of $(n, 2n)$ and (n, n') were unimportant. But in fact $(n, 2n)$ and (n, n') events are reasonably probable. . .
- so almost every neutron, as it repeatedly but ineffectually scatters elastically off of Pb-208, will eventually undergo one of these catastrophic energy loss events and jump to an energy well below the source energy.

This basic mechanism would apply to any heavy nucleus somewhat above the inelastic scatter threshold. But because it is a doubly magic nucleus, Pb-208 has a large excitation energy of 2.61 MeV. Further, at 14 MeV, inelastic scatter from Pb-208 is unusual (at least as modeled in the ENDF-B/VI evaluations) in being dominated by scatter off the first excited state; the inelastic scatter cross section from the second and third excited states is an order of magnitude smaller than for the first excited state. Pb-206, Pb-207 and Bi-209 do not share these characteristics of Pb-208, and while they still show the same large flux depression below a monoenergetic source, it is not quite so deep or dramatic and contains structure due to scattering off of different levels. Pb-208 provides the most dramatic and clean example of the flux depression.

So, for Pb-208 I will ignore inelastic scatter from energy levels higher than the first. Neutrons that inelastically scatter lose at least 2.61 MeV. Conservation of energy also implies that 14 MeV neutrons that undergo $(n, 2n)$ events result in neutrons appearing at energies below 6.63 MeV. Thus neutrons will jump down a long way in energy when they do, almost inevitably, undergo an (n, n') or $(n, 2n)$ event right below source energy. Any neutron that crosses the 2.61 MeV gap from 14 MeV down to 11.4 MeV only by elastic scatter will have to interact *at least* $\log(14/11.4)/\log(\alpha) \approx 11$ times to cross this large energy gap; the probability that a neutron can do so without an inelastic or $(n, 2n)$ event is less than 10^{-3} . And this is the best case for elastic scattering; if scattering is isotropic in the center of mass then roughly 22 elastic scatters would be required, on average, with a probability of only 10^{-6} . In fact, elastic scattering off of Pb-208 is quite forward peaked at 14 MeV, so elastic scattering results in an even smaller neutron energy loss on average, and more than 22 elastic scatters would be required to cross from 14 MeV to 11.4 MeV. This will happen to fewer than 1 in 10^6 particles; the low probability of this elastic crossing results in an extremely wide and deep flux depression as neutrons are removed by catastrophic (n, n') and $(n, 2n)$ events.

This explanation of the flux depression implies that we should see it in any material whose first energy level is much greater than the average energy loss in elastic scatter, provided we start with neutrons above the (n, n') threshold. The depression will be at least as wide as the lowest excitation energy of the nucleus, and the depth of the depression will depend on its width, the average energy

loss in elastic scatter, and the relative probability of elastic scatter compared to catastrophic events like (n, n') and $(n, 2n)$. I will explore this with a simple model in the next section.

3 A MODEL

A model that contains the essential physics for describing the flux depression in Pb-208 can be developed by assuming:

1. a pure, heavy element with mass number $A \gg 1$,
2. on which neutrons can scatter either elastically and isotropically in the center-of-mass, or
3. scatter inelastically off of a single level of energy Q above ground, and
4. on which all other nuclear events such as $(n, 2n)$ remove the neutron from the energy range under consideration.

Starting with a monoenergetic source at energy E_0 I will consider only the energy range from E_0 to a bit below $E_0 - Q$. (Note that $Q > 0$ denotes the energy above ground of the first excited state of the nuclear target, rather than the negative of this value.) This energy range is assumed to be above the (n, n') threshold, and above the maximum neutron energy emitted from a $(n, 2n)$ reaction.

If the elastic scatter is isotropic in the center of mass system, the neutron balance can be written as

$$\Sigma_t \phi(E) = \int_E^{E/\alpha} \frac{\Sigma_{se}(E')}{E'(1-\alpha)} \phi(E') dE' + \int_{E+Q}^{\infty} \Sigma_{(n,n')}(E' \rightarrow E) \phi(E') dE' + S\delta(E - E_0) \quad (1)$$

where $\alpha = (A - 1)^2 / (A + 1)^2 \approx 1$. In reality neutrons in the MeV energy range often forward scatter off of Pb-208, but the key physics that I need is captured here: neutrons slow down via elastic collisions, but not very well, and they also slow down via catastrophic events. To model the inelastic scatter, I take the limit $A \rightarrow \infty$ so that $\Sigma_{(n,n')}(E' \rightarrow E) = \Sigma_{(n,n')}(E') \delta(E' - (E + Q))$, meaning only neutrons with energy $E + Q$ can inelastically scatter to energy E . This simple model still contains the key physics to explain the flux depression for neutrons slowing down in Pb-208 and similar nuclei.

Now note that $\alpha \approx 1$ for heavy elements and make the standard age theory (Beckurts and Wirtz, 1964) expansion

$$E' \Sigma_{se}(E') \phi(E') \approx E \Sigma_{se}(E) \phi(E) + \frac{d}{d \log E} E \Sigma_{se}(E) \phi(E) \log(E'/E) \quad (2)$$

so that the neutron balance now becomes

$$\Sigma_{ne} \phi(E) = \frac{d \xi E \Sigma_{se} \phi(E)}{dE} + \Sigma_{(n,n')}(E + Q) \phi(E + Q) + S\delta(E - E_0) \quad (3)$$

Table 1: Key interaction parameters for neutrons on Pb-208, estimated using $\alpha \approx 0.98$ and $\xi \approx 0.0096$. Note that the value of K is estimated assuming isotropic elastic scatter in the center of mass frame. The best value of K will be smaller because the scatter is actually forward peaked.

Energy	Σ_{se}	Σ_{ne}	K	p
10 MeV	2.800b	2.614b	0.010	0.5271
11.4 MeV	2.814b	2.594b	0.010	0.2957
14 MeV	3.010b	2.611b	0.011	0.1879

where $\xi = 1 + \alpha \log(\alpha)/(1 - \alpha)$ and Σ_{ne} is the nonelastic cross section. For Pb-208 Σ_{ne} and Σ_{se} are both nearly constant.

These approximations leave us with a lean, mean neutron balance model

$$\phi(E) = K \frac{d}{dE} E \phi(E) + p(E + Q) \phi(E + Q) + \mathcal{S} \delta(E - E_0) \quad (4)$$

where the parameter $K = \xi \Sigma_{se} / \Sigma_{ne}$ characterizes the efficiency of slowing down via elastic scatter, $p(E) = \Sigma_{(n,n')}(E) / \Sigma_{ne}$ is the probability that a nonelastic interaction event is an inelastic scatter, and $\mathcal{S} = S / \Sigma_{ne}$. Equation 4 contains two pieces of physics: continuous elastic slowing down of neutrons, and catastrophic slowing down events. Table 1 shows some values of K and p for Pb-208. Note that at these energies $K \ll 1$, indicating that neutrons will lose energy much more effectively in nonelastic events than in elastic scattering, even though elastic scattering is somewhat more probable.

I now develop a few results concerning the solution $\phi(E)$ of this balance equation, starting with a description of the flux depression that appears below the source energy.

Proposition 1 Assume $K, p, Q, E_0, \mathcal{S} > 0$ and $K < 1$. If

$$(1 - K) \left(1 - \frac{Q}{E_0}\right)^{(1-K)/K} < p(E_0)$$

then the flux $\phi(E)$ satisfying Eq. 4 increases monotonically with energy from a local minimum value of

$$\phi(E_0 - Q) = \frac{\mathcal{S}}{E_0 K} \left(1 - \frac{Q}{E_0}\right)^{(1-K)/K}$$

at $E_0 - Q$, up to the value

$$\phi(E_0) = \frac{\mathcal{S}}{E_0 K}$$

at E_0 .

To establish the proposition I first solve the neutron balance equation in the energy range $E_0 - Q < E < E_0$. In this range there is no inelastic inscatter source, and source neutrons simply slow down elastically or are catastrophically removed to a lower energy. The flux in this range will be denoted $\phi_1(E)$, and it satisfies

$$\phi_1(E) = K \frac{d}{dE} E \phi_1(E) + \mathcal{S} \delta(E - E_0). \quad (5)$$

Introducing an appropriate integrating factor, this becomes

$$0 = K \frac{d}{dE} \left[E \phi_1(E) \left(\frac{E_0}{E} \right)^{1/K} \right] + \left(\frac{E_0}{E} \right)^{1/K} \mathcal{S} \delta(E - E_0). \quad (6)$$

Integrating from just above E_0 down to $E \geq E_0 - Q$ yields

$$E \phi_1(E) \left(\frac{E_0}{E} \right)^{1/K} = \mathcal{S}/K \quad (7)$$

which implies

$$\phi_1(E) = \frac{\mathcal{S}}{EK} \left(\frac{E}{E_0} \right)^{1/K}. \quad (8)$$

So, for $0 < K < 1$ this flux goes from a maximum at the source energy

$$\phi_1(E_0) = \frac{\mathcal{S}}{E_0 K} \quad (9)$$

down to a value

$$\phi_1(E_0 - Q) = \frac{\mathcal{S}}{E_0 K} \left(1 - \frac{Q}{E_0} \right)^{(1-K)/K} \quad (10)$$

and it does so monotonically.

To confirm that $E_0 - Q$ is in fact a local minimum we must examine the flux for energies just below $E_0 - Q$. Call the flux $\phi_2(E)$ in the energy range $E_0 - 2Q \leq E \leq E_0 - Q$, and consider the neutron balance

$$\phi_2(E) = K \frac{d}{dE} E \phi_2(E) + p(E + Q) \phi_1(E + Q) \quad (11)$$

for $\phi_2(E)$. Rearranging this yields

$$\frac{d\phi_2}{dE}(E) = \frac{1}{EK} \left[(1 - K) \phi_2(E) - p(E + Q) \phi_1(E + Q) \right] \quad (12)$$

and this can be evaluated at $E = E_0 - Q$, where $\phi_2(E_0 - Q) = \phi_1(E_0 - Q)$, to yield

$$\frac{d\phi_2}{dE}(E_0 - Q) = \frac{\mathcal{S}}{E_0 K} \frac{1}{K(E_0 - Q)} \left[(1 - K) \left(1 - \frac{Q}{E_0} \right)^{(1-K)/K} - p(E_0) \right]. \quad (13)$$

So, if the term in brackets is negative,

$$\left[(1 - K) \left(1 - \frac{Q}{E_0} \right)^{(1-K)/K} - p(E_0) \right] < 0 \quad (14)$$

then the slope of the flux just below $E_0 - Q$ is negative. This implies that the flux does indeed have a local minimum at $E_0 - Q$, and this completes the proof of Proposition 1.

The requirements of Proposition 1 are met for Pb-208 in the 10–14 MeV range; here $K \ll 1$, $p > 0.1$ and $Q/E_0 < 1$, so

$$\left[(1 - K) \left(1 - \frac{Q}{E_0} \right)^{(1-K)/K} - p(E_0) \right] \approx \left[\left(1 - \frac{Q}{E_0} \right)^{1/K} - p(E_0) \right] \approx -p(E_0) < 0. \quad (15)$$

Thus, this model reproduces a deep flux depression, like the one seen in the Monte Carlo simulation. Note also that Eqs. 8, 13 and 15 imply that

$$\left| \frac{1}{\phi} \frac{d\phi}{dE}(E_0 - Q) \right| \approx \frac{p(E_0)}{(E_0 - Q)K} \left(1 - \frac{Q}{E_0} \right)^{-1/K} \gg 1, \quad (16)$$

so at $E_0 - Q$ the flux climbs very rapidly, and the depression thus ends quite suddenly. This is again seen in the Monte Carlo simulation. The increase in flux with decreasing energy below $E_0 - Q$ comes about because the rate of inelastic scatter from E_0 down to $E_0 - Q$ is greater than the rate at which neutrons at $E_0 - Q$ scatter to lower energies, and this occurs because the flux at $E_0 - Q$ is so small.

Of course neutrons slowing down in Pb-208 do not exactly follow Eq. 4, but the behavioral agreement observed between the Monte Carlo simulations and this simple model suggest that the essential physics is there. Using the parameters from Table 1 for 14 MeV results in a flux depression depth

$$\frac{\phi(E_0 - Q)}{\phi(E_0)} = \left(1 - \frac{Q}{E_0} \right)^{(1-K)/K} \approx 10^{-8}. \quad (17)$$

The depth of this flux depression is certainly significant; in fact, the true flux depression should be deeper than shown because K is being over-estimated. We cannot directly determine the depth of the flux depression from the Monte Carlo calculation either, because no neutrons were tallied at the bottom of the depression. But we can estimate an upper bound from the simulation by using the observed depth of the depression at 12.7 MeV, yielding $\phi(11.4 \text{ MeV})/\phi(14 \text{ MeV}) < 2 \times 10^{-8}$, consistent with the estimate of Eq. 17.

However, an effective value of K can be extracted from the Monte Carlo simulation. From Eq. 8 the flux integrated over an energy interval $[E, E_0]$, with $E \geq E_0 - Q$ is easily determined as

$$\int_E^{E_0} \phi(E') dE' = \mathcal{S} [1 - (E/E_0)^{1/K}]. \quad (18)$$

Table 2: Values of the parameter K estimated from the Monte Carlo simulation using flux integrals from 14 MeV down to energy E .

E	13.8	13.6	13.4	13.2	13.0	12.8
K	0.00447	0.00503	0.00530	0.00546	0.00561	0.00561

Since $K \gg 1$ this implies

$$\int_{E_0-Q}^{E_0} \phi(E') dE' \approx \mathcal{S}, \quad (19)$$

and the quantity on the left is directly computed from the Monte Carlo results. This provides a normalization to eliminate \mathcal{S} in Eq. 18, which can then be used to estimate

$$K = \frac{\ln(E/E_0)}{\ln\left(1 - \frac{1}{\mathcal{S}} \int_E^{E_0} \phi(E') dE'\right)}, \quad (20)$$

ideally independent of E . The right hand side of this expression is estimated by the Monte Carlo for various discrete values of E (the bottom of various tally bins); the result are shown in Table 2. The values seem to asymptote to $K \approx 0.0056$, although the value varies from a low of 0.045 to a high of 0.056 depending on the value of E used. The variation is perhaps partially due to fluctuations in the Monte Carlo, but is more surely due to the inconsistency between the slowing down model of Eq. 4 and that implemented in the Monte Carlo code. Figure 2 shows the flux computed by the Monte Carlo (red) and that predicted by Eq. 8 (blue) with $K = 0.0056$, and normalized to the simulation using \mathcal{S} from Eq. 19. They match quite well, and the result suggests that the flux depression could be 15 orders of magnitude below the flux at the source energy.

4 BELOW $E_0 - Q$

A close examination of the Monte Carlo simulation will reveal several local maxima and minima of the flux somewhat below the energy $E_0 - Q$; these are most easily seen in Fig. 2. These are not Monte Carlo fluctuations; below 11.4 MeV all flux tallies have relative standard deviations of less than 0.5%. While below $E_0 - Q$ the model in Eq. 4 is on shaky ground, it does capture the first flux peak in this energy range. A rigorous result on this is:

Proposition 2 *If, in addition to the conditions of Proposition 1, $p(E)$ is monotonically decreasing and $p(E_0 - Q) + K < 1$, then the flux $\phi(E)$ satisfying Eq. 4 will have a local maximum at some energy E_m , with $E_0 - 2Q < E_m < E_0$.*

I established above that $d\phi/dE < 0$ at $E_0 - Q$. I shall now establish that, under the conditions of Proposition 2, $d\phi/dE > 0$ at $E_0 - 2Q$. The existence of a point E_m where $d\phi/dE = 0$, with $E_0 - 2Q < E_m < E_0 - Q$, and hence Proposition 2, then follows.

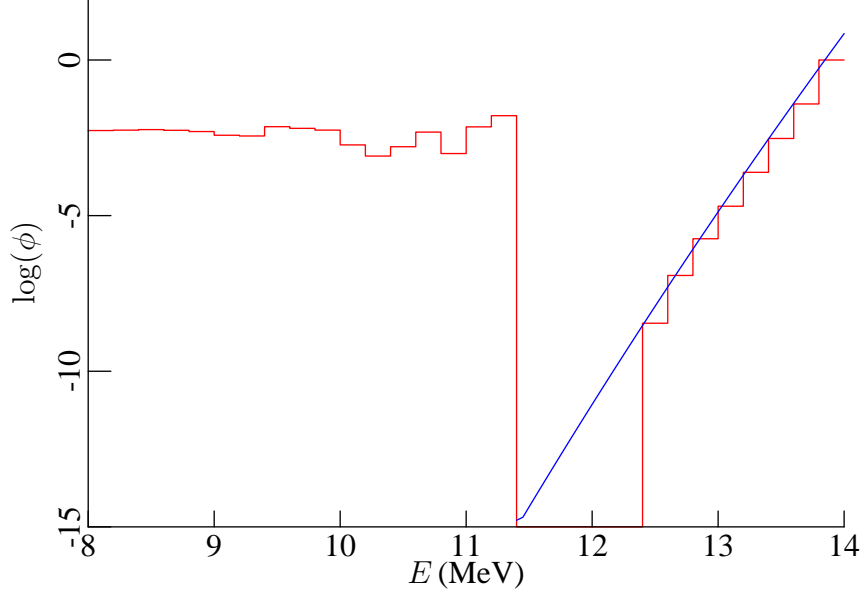


Figure 2: The neutron spectrum near the source energy, generated by 14 MeV neutrons slowing down in Pb-208. Red line: computed using 2×10^8 particles in MCNP. Blue line: computed from Eq. 8 with $K = 0.0056$. Recall that in those regions of phase space where the Monte Carlo results are absent there were *no* simulation particles.

Equation 12 at $E = E_0 - 2Q$ gives us

$$\frac{d\phi_2(E_0 - 2Q)}{dE} = \frac{1}{K(E_0 - 2Q)} \left[(1 - K)\phi_2(E_0 - 2Q) - p(E_0 - Q)\phi_1(E_0 - Q) \right] \quad (21)$$

and so

$$\frac{d\phi_2(E_0 - 2Q)}{dE} = \frac{\phi_1(E_0 - Q)}{K(E_0 - 2Q)} \left[(1 - K) \frac{\phi_2(E_0 - 2Q)}{\phi_1(E_0 - Q)} - p(E_0 - Q) \right]. \quad (22)$$

The sign of $d\phi_2/dE$ at $E_0 - 2Q$ can therefore be determined by developing a lower bound on

$$(1 - K) \frac{\phi_2(E_0 - 2Q)}{\phi_1(E_0 - Q)}. \quad (23)$$

To do so, let us first formally integrate Eq. 11 using the flux-continuity initial condition $\phi_2(E_0 - Q) = \phi_1(E_0 - Q)$, yielding

$$\begin{aligned} \phi_2(E_0 - 2Q) = & \left(\frac{E_0 - 2Q}{E_0 - Q} \right)^{(1-K)/K} \phi_1(E_0 - Q) + \\ & \frac{1}{K(E_0 - 2Q)} \int_{E_0 - 2Q}^{E_0 - Q} \left(\frac{E_0 - 2Q}{E'} \right)^{1/K} p(E' + Q)\phi_1(E' + Q) dE'. \end{aligned} \quad (24)$$

This is not explicitly useful because even for constant p but arbitrary K the integral cannot be evaluated in terms of elementary functions (leaving Hypergeometric out of the class “elementary”). However, from this we have

$$(1 - K) \frac{\phi_2(E_0 - 2Q)}{\phi_1(E_0 - Q)} = (1 - K) \left(\frac{E_0 - 2Q}{E_0 - Q} \right)^{(1-K)/K} + \frac{(1 - K)}{K(E_0 - 2Q)} \int_{E_0 - 2Q}^{E_0 - Q} \left(\frac{E_0 - 2Q}{E'} \right)^{1/K} p(E' + Q) \frac{\phi_1(E' + Q)}{\phi_1(E_0 - Q)} dE'. \quad (25)$$

Now, using the monotonic decrease of $p(E)$ and because under the integral $\phi_1(E' + Q) \geq \phi_1(E_0 - Q)$ we have

$$(1 - K) \frac{\phi_2(E_0 - 2Q)}{\phi_1(E_0 - Q)} > (1 - K) \left(\frac{E_0 - 2Q}{E_0 - Q} \right)^{(1-K)/K} + \frac{p(E_0 - Q)(1 - K)}{K(E_0 - 2Q)^{(K-1)/K}} \int_{E_0 - 2Q}^{E_0 - Q} \left(\frac{1}{E'} \right)^{1/K} dE'. \quad (26)$$

The integral on the right hand side can now be evaluated

$$\int_{E_0 - 2Q}^{E_0 - Q} \left(\frac{1}{E'} \right)^{1/K} dE' = \frac{K}{K - 1} [(E_0 - Q)^{(K-1)/K} - (E_0 - 2Q)^{(K-1)/K}] \quad (27)$$

and so

$$(1 - K) \frac{\phi_2(E_0 - 2Q)}{\phi_1(E_0 - Q)} > (1 - K) \left(\frac{E_0 - 2Q}{E_0 - Q} \right)^{(1-K)/K} + p(E_0 - Q) \left[1 - \left(\frac{E_0 - 2Q}{E_0 - Q} \right)^{(1-K)/K} \right] \quad (28)$$

or

$$(1 - K) \frac{\phi_2(E_0 - 2Q)}{\phi_1(E_0 - Q)} > p(E_0 - Q) + \left(\frac{E_0 - 2Q}{E_0 - Q} \right)^{(1-K)/K} [1 - K - p(E_0 - Q)]. \quad (29)$$

Using this in Eq. 22

$$\frac{d\phi_2(E_0 - 2Q)}{dE} > \frac{\phi_1(E_0 - Q)}{K(E_0 - 2Q)} \left(\frac{E_0 - 2Q}{E_0 - Q} \right)^{(1-K)/K} [1 - K - p(E_0 - Q)] \quad (30)$$

This is positive provided $1 - K - p(E_0 - Q) > 0$, and this establishes Proposition 2.

For 14 MeV neutrons slowing down in Pb-208 the conditions required for Proposition 2 are also satisfied, and so, for parameters characteristic of Pb-208, the simple model being considered here will display a local flux maximum in the energy interval $E_0 - 2Q < E < E_0 - Q$. The appearance of such a local flux maximum in the Monte Carlo simulations might once again suggest that the simple model does indeed contain the essential physics that leads to both the flux depression within one Q below the source energy and the nonmonotonic behavior between Q and $2Q$ below the source energy.

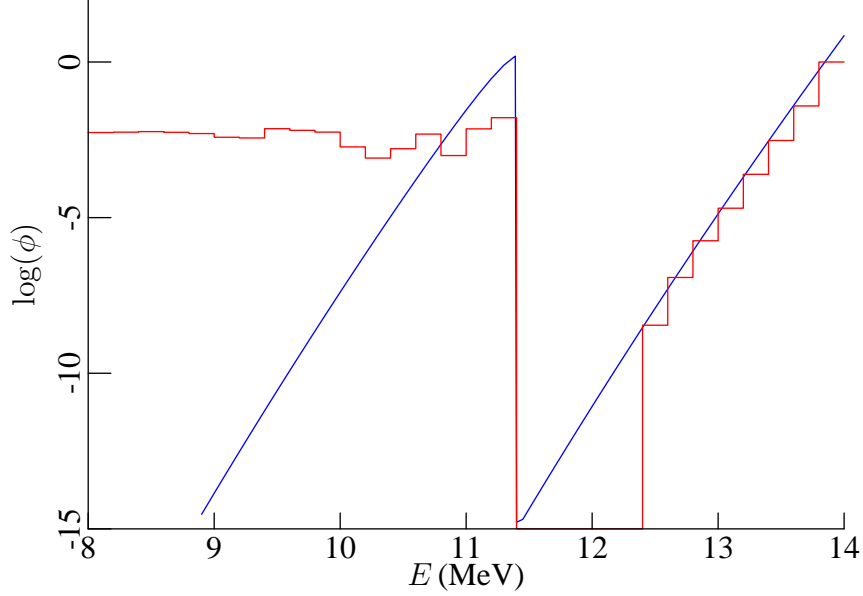


Figure 3: The neutron spectrum near the source energy, generated by 14 MeV neutrons slowing down in Pb-208. Red line: computed using 2×10^8 particles in MCNP. Blue line: computed from the simple model with $K = 0.0056$ and $p = 0.2957$. Note that the modeled flux (blue) is not discontinuous at 11.4 MeV, but it does change very rapidly there.

However, the picture is not actually so clear. The energy $E_0 - 2Q \approx 8.78$ MeV for Pb-208, and the Monte Carlo simulations do not support the assertion of Proposition 2, that the flux is increasing there. Figure 3 compares the flux computed by the Monte Carlo to that from the model, using a constant $p = 0.2957$ (the model solution was computed by introducing an integrating factor for Eq. 11 and computing the resulting integral numerically). The lack of agreement is too great to be due to the variation of p . Rather it is due to the physics missing from Eq. 4.

The large peak just below 11.4 MeV is due to source energy neutrons inelastically scattering off the first excited state. While the model, Eq. 4, assumes that all these neutrons lose an energy of exactly Q , reality is that some lose a bit more. This accounts for the broader, lower peak seen in the Monte Carlo simulation. Further, Pb-208 has as second excited state with energy 3.2 MeV above ground, which will drop source energy neutrons at and below 10.8 MeV. The peak in the Monte Carlo results between 10.6 and 10.8 MeV corresponds to this second excited state of lead. The third excited state would manifest itself at 10.5 MeV, and is probably also contributing to the second flux peak. Thus, below $E_0 - Q$ the effects of the higher energy levels are becoming important, and fill in the secondary flux depression that Eq. 4 would otherwise suggest. In fact, we cannot expect the predictions of Eq. 4 to be correct below an energy E_0 minus the energy of the second excited state (that is, below 10.8 MeV in the current case).

It is not possible at present to quantitatively assess the importance of these physical deficiencies in modeling the flux depression in Pb-208. However, it is worth noting that an important difference between this flux depression in Pb-208 and in other heavy nuclides such as Bi-209 is that the flux

depression in Pb-208 has very little structure, while in Bi-209 simulations show a great deal of structure because multiple excited states of the nucleus are playing equally important roles. In Bi-209 the width of the depression is roughly the energy of the third excited state of the nucleus, but inside the depression are other extreme points whose spacing matches the energy of the first and second excited states.

5 CONCLUSIONS

I have shown in this paper that the combination of small energy loss in elastic scatter and catastrophic energy loss in (n, n') and other nonelastic events can result in a very deep flux depression just below the source energy for monoenergetic neutrons released above the inelastic scatter threshold in heavy moderators. I have focused on Pb-208 because the flux depression caused by slowing down in this material has the simplest structure, but similar deep depressions can be seen for 14 MeV neutrons slowing down in other heavy nuclides, such as Pb-207, Pb-206 and Bi-209. These flux depressions can be very deep (some 15 orders of magnitude for 14 MeV neutrons in Pb-208), and could therefore have a significant impact on the generation of multigroup constants to describe 14 MeV neutron experiments in heavy moderators, such as might be undertaken for ATW integral experiments.

The simple model devised here to describe this flux depression captures its essential features, but misses many details because of some absent physics. It's success at capturing the very deep depression just below the monoenergetic source energy suggests that it could be successfully extended to capture more of the details. A better model of the angular distribution in elastic scatter could be included and inelastic scatter off of other levels could be included. But as we do so the model comes more-and-more to provide the fidelity of Monte Carlo while losing the analytical explanatory power that a simple model provides.

ACKNOWLEDGEMENTS

This research was supported in part by the ATW project under grant number 12987-001-00 3G from Los Alamos National Laboratory.

REFERENCES

- Abánades, A., *et al.*, 1995. Experimental verification of neutron phenomenology in lead and transmutation by adiabatic resonance crossing in accelerator driven systems. *Physics Letters B* **348**, 697–709.
- Andriamonje, S., *et al.*, 1995. Experimental-determination of the energy generated in nuclear cascades by a high-energy beam. *Physics Letters B* **348**, 697–709.
- Bacher, P., 1999. C. rubbia's hybrid plant concept: a preliminary technical and economic analysis. *Nuclear Engineering and Design* **187**, 185–196.
- Beckurts, K. H., Wirtz, K., 1964. *Neutron Physics*. Springer-Verlag.

- Briesmeister, J. F., ed., 2000. *MCNP – A General Monte Carlo N-Particle Transport Code*. No. LA-13709-M. Los Alamos National Laboratory.
- Carminati, F., Géles, C., Klapisch, R., Revol, J. P., Roche, C., Rubio, J., Rubbia, C., 1993. An energy amplifier for cleaner and inexhaustible nuclear energy production driven by a particle beam accelerator. Tech. Rep. CERN/AT/93-47 (ET), CERN.
- Chadwick, M. B., *et al.*, 1999. Cross-section evaluations to 150 MeV for accelerator-driven systems and implementation in MCNPX. *Nuclear Science and Engineering* **131**, 1.
- Gromov, B. F., Orlov, Y. I., Toshinskii, G. I., Chekunov, V. V., 1996. Nuclear power plants with lead-bismuth coolant. *Atomic Energy* **81**, 770–775.
- Gromov, B. F., *et al.*, 1997. Use of lead-bismuth coolant in nuclear reactors and accelerator-driven systems. *Nuclear Engineering and Design* **173**, 207–217.
- Van Tuyle, G., *et al.*, 2001. A roadmap for developing ATW technology: System scenarios & integration. *Progress in Nuclear Energy* **38**, 3–23.
- Waters, L., ed., 1999. *MCNPX User's Manual*. No. TPO-E83-G-UG-X-00001. Los Alamos National Laboratory.